Functional Gene Array-Based Analysis of Microbial Community Structure in Groundwaters with a Gradient of Contaminant Levels

Patricia J. Waldron[1,2], Liyou Wu[1,2], Joy D. Van Nostrand[1,2], Chris W. Schadt[2,3], David B. Watson[2,3], Philip M. Jardine[2,3], Anthony V. Palumbo[2,3], Terry C. Hazen[2,4], Jizhong Zhou[1,2*]

[1]*Institute for Environmental Genomics, University of Oklahoma, Norman, OK*

[2]*Virtual Institute for Microbial Stress and Survival, http://vimss.lbl.gov*

[3]*Oak Ridge National Laboratory, Oak Ridge, TN*

[4]*Lawrence Berkeley National Laboratory, Berkeley, CA*

*For correspondence. E-mail jzhou@ou.edu; Tel (+1) 405 325 6094; Fax (+1) 405 325 7552

Summary

Six groundwater monitoring wells from the Field Research Center of the U.S. DOE Environmental Remediation Science Program (ERSP) at Oak Ridge, TN, were selected to compose a gradient of pH, nitrate and heavy metal contamination. DNA from the groundwater bacterial community was analyzed with a functional gene array containing 2,006 probes for the detection of genes involved in metal-resistance, sulfate-reduction, contaminant degradation and carbon and nitrogen cycling. Diversity decreased in relation to the level of contamination within each well, and each community exhibited a different distribution of genes. Heatmaps of metal resistance genes and *nirK* and *nirS* genes indicate that highly contaminated wells had lower gene diversity, but greater signal intensity for detected genes. Wells with the highest sulfate concentrations had the greatest diversity and signal intensity for *dsrAB* genes. A greater number of carbon fixation genes (*cbbL*, *cbbM*) were detected than fermentation genes (FTHFS) in all wells. A variety of organic contaminant degradation genes were also detected. Results of Mantel tests and canonical correspondence analysis indicate that nitrate, sulfate, pH, uranium and technetium have a significant ($p < 0.05$) effect on bacterial community structure. This study provides an overall picture of bacterial community structure in contaminated environments across many different functional genes and shows that diversity can vary widely in relation to the degree of contamination.

Introduction

Environmental contaminants can have large and complex impacts on bacterial community structure, and understanding these impacts will facilitate better management of

microbial communities for bioremediation. Detection, characterization and quantification of microorganisms in natural settings, however, are very challenging endeavors. And establishing links between microbial diversity and ecosystem functions presents even more challenges. Functional gene arrays (FGAs), or GeoChips, allow simultaneous detection of thousands of populations of bacteria (Wu *et al.*, 2007, Rhee *et al.*, 2004, Tiquia *et al.*, 2004; He *et al.*, 2007). Here we report using an FGA with ~2000 gene probes to examine the impacts of contaminants on bacterial community structure in a contaminated site. It is expected that, by correlating gene diversity with geochemistry, we can better understand which variables are most important in determining bacterial community structure, and how that community changes along an environmental gradient.

The Oak Ridge, TN Field Research Center (FRC) established by the Department of Energy is the site of extensive research in the bioremediation of heavy metals due to legacy contamination from Cold War era uranium (U) enrichment (Oak Ridge National Laboratory, 2008). The former S-3 waste ponds located at the Y-12 Security Complex received large quantities of waste containing radionuclides, nitric acid, and various organic solvents, until their closure in 1983. These unlined ponds are the source of a contaminant plume traveling through the groundwater that has resulted in gradients of U, technetium (Tc), nitrate and pH throughout the area. The contaminants alter local bacterial populations by exerting selective pressure (Akob *et al.*, 2007), but leave other populations intact (Bagwell *et al.*, 2006). Many studies of this site have used culturing techniques (M. Fields *et al.*, 2005; Spain *et al.* 2007) and molecular biomarker analysis (Palumbo *et al.*, 2004; Bagwell *et al.*, 2006; Yan *et al.*, 2003; Akob *et al.*, 2007, Spain *et al.* 2007) to examine the bacterial diversity and functional capabilities of bacteria present in the area, but none of these studies have been able to simultaneously examine the

diversity of multiple functional genes. The objective of this study is to examine the bacterial community structure in wells of varying contamination and to determine which contaminants have the greatest effects on bacterial diversity. Our results indicate that metal and nitrate contamination have significant effects on bacterial community composition at the Oak Ridge FRC. Tc, nitrate, U, sulfate and pH were all shown to have a significant correlation with bacterial gene diversity, as determined by Mantel tests, and canonical correspondence analysis (CCA).

Results and Discussion

Description of Gene Diversity

DNA was extracted from groundwater from selected monitoring wells, amplified by whole community genome amplification and labeled with a fluorescent dye. The DNA was hybridized to the FGA overnight, and the arrays were scanned to identify positive genes. The FGA detected a number of genes with high signal intensity from each well (111 to 302 genes per sample) (Wu, 2006). Overall, gene diversity was lower in more contaminated wells than in pristine and low-contamination wells, and the Simpson's genetic diversity index reflects this trend (Wu, 2006). This trend has also been observed in 16S clone libraries from FRC groundwater (Fields, 2005) and is likely the result of contaminant stress reducing the numbers of species that can survive in this polluted environment. Wells with less contamination also had higher percentages of unique genes (11-20%) than high contamination wells (5%), except for well FW024, which had 16% unique genes (data not shown).

General differences in community structure can be seen in Fig. 1. The percentage of genes detected is standardized by dividing by the number of probes printed on the slide. All

gene categories are represented in all wells, though percentages of each category differ by well. For example, FW-024, FW-010 and TPB-16 have higher percentages of genes related to sulfate-reduction, while FW-021, FW-003 and FW-300 have higher percentages of contaminant degradation genes.

Functional Gene Populations

Heatmaps of individual functional gene groups (Fig. 2) clustered the wells into very similar groupings. For comparison purposes, wells FW-003, FW-300 and FW-021 are designated as group A, while FW-010, FW-024 and TPB-16 are designated as group B. The consistency of the grouping throughout all heatmaps shows the importance of geochemistry across all populations of bacteria. Wells FW-003, FW-300, and TPB-16 were expected to group together as "low-contaminant" wells, and FW-010, FW-024 and FW-021 as "high-contaminant wells" but TPB-16 and FW-021 grouped contrary to expectations. Several possibilities may explain these exceptions, including differences in soil type and composition between the different areas sampled at the FRC, disparities in hydrogeology between the wells and bioegeographical variation. Levels of toxic organic contaminants and the presence of organic carbon to support bacterial growth, which were not measured in this study, may also play a role in determining the composition of the bacterial community that was observed.

In the metal-resistance heatmap (Fig 2a), the genes with the greatest signal intensity were a grouping of arsenate-, tellurite- and mercury-resistance genes that were present in both low and high contaminant-level wells: FW-024, FW-021, FW-300, and FW-003 (Fig. 2a). Very few metal-resistance and transport genes were detected from wells FW-010 and TPB-16, despite the high levels of aluminum (Al), nickel (Ni) and Tc in FW010, and moderate Tc and U contamination in TPB16 (Table 1). Both wells had the lowest total gene numbers detected, and

so the lack of metal-resistance genes may simply be the result of low diversity, and may not actually reflect the importance of metal-resistance genes in these wells. A tellurite resistance gene (*telA*) (Walter *et al.*, 1991) and a cation efflux system gene (*czcA*) that exports the redox-inactive metals Co, Zn and Cd, from several types of bacteria (Nies, 2003) was found to be prevalent in all wells tested.

Sulfite-reductase genes (*dsrAB*) were most prevalent in the well with the highest sulfate concentration FW-024 (987.1 $mg^{-1}l$ sulfate) (Fig. 2b). FW-300 (6.4 $mg^{-1}l$ sulfate) has a surprisingly high diversity of *dsrAB* genes, considering its low of sulfate concentration. Notably, a gene similar to the sulfite reductase from *Desulfovibrio desulfuricans*, a bacterium capable of Tc reductation (Lloyd *et al.*, 1998), was detected in FW-003, which has a moderately-low level of Tc (141.0 $pCi^{-1}l$). The presence of this type of bacteria may be important for successful bioremediation of this area.

Despite the differences in their geochemistry, Group B, TPB-16, FW-024 and FW-010, have very similar *dsrAB* diversity and high signal intensity (Fig. 2b). Well TPB-16 has a moderate contaminant load, and sulfate concentration (116.1 $mg^{-1}l$) and is located near a zero-valent iron reactive barrier that was installed for the purpose of passively remediating the soil (Bagwell, 2006). Increased sulfate reduction has been observed close to the barrier at this site, and in other Fe^0 barriers (Gu, 2002; Gu, 1999; Phillips, 2002). Well FW-010 (8.3 $mg^{-1}l$ sulfate) also clusters closely within this group despite its low sulfate concentration. FGA results suggest that certain *dsr* genes from uncultured organisms are prevalent in well FW-010, as well as a *Desulfobacterium*-like *dsr* gene, and one sequenced from the contaminated Shiprock, NM Uranium Mill Tailings Remedial Action (UMTRA) site (Chang *et al.*, 2001).

The presence of sulfate-reducing bacteria in these wells is important because they may play an important role in reducing and stabilizing metals during bioremediation. Several sulfate-reducing bacteria can use U(VI) as an electron acceptor (Lovley and Phillips, 1992; Beyenal *et al.*, 2004), transforming it into insoluble U(IV) and can generate uranium sulfides through the production of H_2S (Hua *et al.*, 2006). A study looking at SRB diversity in U-contaminated groundwater found significant relationships between the abundance of *Desulfotomaculum* and *Desulfotomaculum*-like organisms and the concentration of sulfate and U in the groundwater (Chang *et al.*, 2001). The researchers speculated that the increase in *Desulfotomaculum* with increasing U concentrations was indicative of a competitive advantage conferred by the U, either through *Desulfotomaculum*'s U-resistance or its use of U(VI) as a terminal electron acceptor. Though *dsr* genes similar to *Desulfovibrio desulfuricans*, a known U-reducing organism (Lovley and Phillips, 1992, Payne *et al.*, 2002), and *Desulfotomaculum*, a group that is prevalent at the Shiprock, NM UMTRA site [U(IV) concentrations up to 2.85 $mg^{-1}l$] (Chang, *et al.*, 2001), were detected in this study; the highest signal intensities were from *dsr* sequences from uncultured lab clones (fig. 2b). Several of these *dsrAB* sequences were from previous studies of *dsrAB* diversity in FRC wells FW-300, FW-010, FW-005 and FW-003. These results indicate that the FGA is capable of detecting genes that are expected to be present at the FRC, but suggest that many of the SRB at this site have not been cultured, indicating a need for further study of these organisms.

The nitrite reductase genes (*nirS* and *nirK*) detected in this study grouped the wells into clusters similar to those in the metal resistance and *dsrAB* heatmaps (Fig. 2c). Generally, Group B had lower diversity than Group A, but the individual genes had higher signal intensities. This would be expected in environments where low pH and high metal concentrations would select

for a few resistant, denitrifying bacteria, thus lowering the total diversity and evenness, as indicated by a previous study at the FRC (Fields *et al.*, 2005). Like the dsrAB genes, most of the *nirS* and *nirK* sequences detected were from uncultured bacteria from environmental samples.

Other studies have found differences in *nirS* and *nirK* diversity in FRC wells. Higher *nirK* diversity was detected in wells with extremely high nitrate concentrations, while higher *nirS* diversity was detected in low nitrate wells (Yan *et al.*, 2003). Greater *nirS* diversity was also detected in clone libraries from wells stimulated with ethanol in Area 2 (Spain *et al.*, 2007). Our results show approximately equal numbers of *nirS* and *nirK* genes in each well (Fig. 2c). In some wells, the *nirS* signal intensities were several fold greater than the intensity of *nirK*, indicating a greater abundance of those genes in the sample (data not shown), however, the differences do not appear to correlate with nitrate concentration.

Carbon utilization is also an important process at the FRC because carbon is severely limited in this environment. To detect the presence of carbon fixation genes, probes for ribulose 1,5-bisphosphate carboxylase (Rubisco, specifically, *cbbL*, *cbbM*), which has been used a biomarker for the Calvin Benson-Bassham CO_2 fixation pathway (Campbell and Cary, 2004), are present on the array. Though Rubsico is commonly associated with phototrophy, a variety of chemolithotrophs and mixotrophs also use Rubisco for CO_2 fixation (Badger and Bek, 2008). Probes for formyltetrahydrofolate synthetase (FTHFS) are also present to detect acetogenic, fermentative bacteria (Leaphart and Lovell, 2001). The heatmap of Rubisco and FTHFS genes show distinct groups of genes that are present throughout all the wells, such as a sequence similar to the Rubisco gene from *Methylococcus capsulatus*, and some that are only present in one group or the other (Fig. 2d). A gene similar to the *Synorhizobium meliloti* Rubisco gene was detected in Group A, while Rubisco genes similar to several uncultured environmental species

were detected in Group B Though FTHFS and Rubsico are present in each well, more Rubisco genes and with higher signal intensities were detected than fermentation genes, despite a greater number of FTFHS probes on the array. Due to the limited carbon available in this environment, chemolithoautotrophy may be a more important process than fermentation in this environment, but activity measurements must be done to confirm these results.

A large variety of organic contaminant degradation genes were detected in the FRC wells (Fig. 2e). Besides nitrate and heavy metals, the FRC is also contaminated with organic solvents, most notably, trichloroethylene (TCE). Several species of bacteria are able to degrade TCE to dichloroethylene (DCE) and vinyl chloride, and these activities have been observed previously at the FRC (Lenczewski *et al.*, 2003). A heatmap of the most abundant and relevant organic contaminant degradation genes was constructed. The greatest diversity of genes was observed in wells FW-300 and FW-003, and the highest total signal intensity was detected in FW-300 and FW-024. The degradation genes most often detected were for common aromatic compounds, and their intermediates, including benzoate, biphenyl, catechol, naphthalene, and phenol.

When looking specifically at TCE degradation genes, there is greater diversity in the wells with low or background-level organic contaminants (FW-300, FW-003). However, FW-021 and FW-024 have the highest average intensity for the TCE genes present, indicating an abundance of these few genes. No TCE degradation genes were detected in FW-010, despite significant levels of TCE and other organic compounds measured at this site (Oak Ridge National Laboratory, 2008). No TCE degradation genes were detected in TPB-16, which has no detectable TCE.

Relationship between gene diversity and groundwater geochemistry

BioEnv was used to find the highest Spearman rank correlation between the measured variables and the species composition (Clarke and Ainsworth, 1993). Sulfate, pH, Al and Tc were identified as the combination of environmental variables that gives the best correlation ($r = 0.8036$) of environmental factors with the bacterial community. The combination of these geochemical variables has a strong, positive correlation with the community structure. Mantel tests were also performed to correlate functional gene composition of the wells with the measured environmental variables (Table 2). Of all the geochemical variables, only nitrate ($p = 0.0270$, $r = -0.255$) and U ($p = 0.0491$, $r = -0.233$) produced significant correlations with the detected functional genes.

The top five geochemical variables identified by automatic forward selection were examined by CCA for correlation with community composition (Fig. 3). Due to the multicollinearity of the variables, U and Tc were combined ($r = 0.922$) and nitrate was removed to reduce inflation. The first axis explained 47.3% of the bacterial diversity observed, and the second axis explained 14.3% of the diversity, describing 61.6% of the total variation. Generally the CCA divided the wells into a low-contamination group (FW-300 and FW-003), and a high contamination group (FW-010 and FW-024), with TPB-16 and FW-021 by themselves. The bacterial diversity present in FW-010 and FW-024 appears to be strongly affected by the sulfate, Tc and U concentrations in those wells, as indicated by their proximity to the combined Tc and U arrow, and the sulfate arrow. The community structure in wells FW-300 and FW-003 appear to be mainly affected by their circumneutral pH. Well FW-021 and TPB16 are not close to any of the geochemical arrows, indicating that unmeasured factors are likely to be the important controllers of bacterial diversity in these wells. The CCA had high species-env. correlations (Table 3) and the combination of all canonical axes was significant ($p = 0.041$). Similar to

results in the present study, Palumbo *et al.* (2004) identified U, sulfate, and pH, as well as Tc and nitrate as important geochemical variables in a PCA of *dsrAB* genes.

Variation partitioning analysis was performed to attribute the variation observed in the bacterial community composition and abundance to the environmental variables identified to be most important by CCA (Fig. 4). Three variables explained a large portion of the variation observed, leaving 45.1% of the variation unexplained by these factors. pH alone explained 21.4%, ($p = 0.175$), 12.4% of the variation was attributed to sulfate ($p = 0.006$) and Tc and U explained the largest amount of variation, 21.2% ($p = 0.086$). Interactions between pairs of variables explained smaller amounts of variation, except for the interaction between sulfate and Tc and U, which accounted for 18.7% of the variation observed. This interaction may be explained by the ability of many sulfate-reducing bacteria to also reduce U and Tc, and the presence of sulfate in the metal-contaminated wells. None of the variation was attributed to the interaction of all three variables.

Summary and conclusions

A variety of genes involved in metal-, sulfate- and nitrate-reduction were detected by the functional gene array in all wells sampled, even those with the highest contaminant levels. Multiple organic contaminant degradation genes were also detected, and these results are promising for the application of bioremediation to the site. This study indicates that metal, sulfate and nitrate contamination have significant effects on bacterial diversity at the Oak Ridge FRC. Tc, U, nitrate, sulfate and pH were all shown to have a significant correlation with bacterial gene diversity, as determined by Mantel tests and CCA. The moderate correlations with geochemical variables indicate that the factors determining bacterial diversity are more complex than the simple presence or absence of a contaminant, and the interactions between

these variables also have an effect on community structure. There are also likely to be synergistic effects between contaminants and natural environmental factors on determining bacterial community structure, such as the effect of carbonate concentrations on U sorption and mobility (Zhou and Gu, 2005) which may affect toxicity and reduction rates. Also, in this study, the FGA was used to detect the relative abundance of multiple bacterial functional groups, but these results do not indicate bacterial activity. Quantifying which bacteria are functional, may give a stronger correlation with the well geochemistry.

As this study demonstrates, functional gene microarrays are ideal for monitoring changes in bacterial populations in time and space as they can detect a variety of bacterial populations at different levels of specificity and have high-throughput capabilities. The results of this study indicate a relationship between environmental variables and community structure that is more complex than general measurements of diversity and bacterial abundance. Future studies may be done to determine how these communities change with time and how they are affected by bioremediation technologies.

Experimental Procedures

Site description

The Oak Ridge FRC (Oak Ridge, TN) is divided into five contaminated areas flanking the former waste ponds, as well as an uncontaminated background site, located approximately 2 km away. For a complete description of the extent of contamination, geochemistry and hydrogeology of the area, see http://www.esd.ornl.gov/orifrc/. Six groundwater monitoring wells at the FRC, varying in distance from the former waste ponds, were selected for sampling (Table 1).

Functional Gene Microarray Description

To examine bacterial communities in the selected wells, a functional gene array was employed. The FGA is a 50-mer oligonucleotide array consisting of 2,006 probes for a variety of genes involved in carbon, nitrogen, sulfur and phosphorus cycling, metal resistance and organic contaminant degradation (Wu, *et al.*, 2006, Rhee *et al.* 2004, Tiquia *et al.*, 2004, Wu *et al.* 2008). The array also contains 16S rRNA gene positive control spots, as well as six human genes and four plant genes as negative controls. Each probe is printed in duplicate.

DNA extraction, amplification, labeling and hybridization

Groundwater (2L) was collected from the selected monitoring wells and shipped to the lab. Bacteria were collected by centrifugation and high molecular weight DNA was extracted from the cell pellets using a previously described method (Zhou *et al.*, 1995). The DNA pellets were dissolved in 20 ul of water. Nanogram amounts of community DNA (1 ul) were amplified using whole community genome amplification (WCGA) (Templiphi kit, Amersham Biosciences, Piscataway, NJ) (Wu *et al.*, 2006) and then labeled with a Cy5 fluorescent dye (GE Healthcare, Piscataway, NJ) using a random priming method (Tiquia, *et al.*, 2004, Rhee *et al.* 2004). FGA slides were sealed inside individual flow cells (Telechem International) and the labeled DNA was hybridized at 50 ºC overnight. After hybridization, arrays were washed in buffer and air dried.

Microarray scanning, data processing and analysis

Arrays were scanned with a ScanArray 5000 microarray analysis system (Perkins-Elmer, Wellesley, MA) and digitally analyzed using ImaGene (Biodiscovery Inc., Los Angeles, CA). Spots with a signal to noise ratio [SNR = (signal intensity – background intensity)/standard deviation of the background] (Verdnik *et al.*) greater than 2 were used for further analysis. Gene

diversity analysis was performed using the hierarchical clustering algorithm in CLUSTER and was visualized using TREEVIEW (Eisen *et al.*, 1998). Geochemical analysis of groundwater pH, and metal and ion concentrations was provided by the FRC, and data was normalized by square root transformation prior to analysis. A BioEnv analysis was performed on the geochemical and gene diversity matrices generated for the wells using the vegan package in R (R Development Core Team, 2008). BioEnv finds the best Spearman rank correlation of the Euclidean distances of scaled environmental factors, with the observed community dissimilarities. Mantel tests (Mantel, 1967) for linking geochemistry and diversity were performed using PC-ORD v. 5.0 (McCune, B. and M. J. Mefford. 1999 MjM Software, Gleneden Beach, Oregon). Canonical correspondence analysis (CCA) (Hotelling, 1936) and partial CCA (pCCA) were performed using CANOCO (ter Braak, 1998). Of all the variables measured, four geochemical variables, U combined with Tc, pH, and sulfate were selected for CCA with microarray hybridization signal intensities based on automatic forward selection of the variables in CANOCO, and their inflation factors. pCCA was used to partition variation in community composition to these geochemical variables.

Acknowledgements

The authors would like to Sanghoon Kang for valuable assistance in data analysis. This research was supported by The United States Department of Energy under the Environmental Remediation Science Program, under Contract No. DE-AC02-05CH11231, and the Genomics:GTL program through the Virtual Institute of Microbial Stress and Survival (VIMSS; http://vimss.lbl.gov).

References

Akob, D.M., H.J. Mills, J.E. Kostka. (2007) Metabolically active microbial communities in uranium-contaminated subsurface sediments. *FEMS Microbiol Ecol* **59**: 95-107.

Badger, M.R., E.J. Bek. (2008) Multiple Rubisco forms in proteobacteria: their functional significance in relation to CO2 acquisition by the CBB cycle. *J Exp Bot* Advanced access Feb. 2, 2008: 1-17.

Bagwell, C.E., X. Liu, L. Wu, J. Zhou. (2006) Effects of legacy nuclear waste on the compositional diversity and distributions of sulfate-reducing bacteria in a terrestrial subsurface aquifer. *FEMS Microbiol Ecol* **55**: 424-431.

Beyenal, H., R.K. Sani, B.M. Peyton, A.C. Dohnalkova, J.E. Amonette, Z. Lewandowski. (2004) Uranium Immobilization by Sulfate-Reducing Biofilms. *Environ Sci Technol* **38**: 2067-2074.

Campbell, B.J., S.C. Cary. (2004) Abundance of reverse tricarboxylic acid cycle genes in free-living microorganisms at deep-sea hydrothermal vents. *Appl Environ Microbiol* **70**: 6282–6289.

Chang, Y.J., A.D. Peacock, P.E. Long, J.R. Stephen, J.P. McKinley, S.J. McNaughton, A.K.M.A. Hussain, A.M. Saxton, D.C. White. (2001) Diversity and characterization of sulfate-reducing bacteria in groundwater at a uranium mill tailings site. *Appl Environ Microbiol* **67**: 3149-3160.

Clarke, K.R., M. Ainsworth. (1993) A method of linking multivariate community structure to environmental variables. *Mar Ecol-Prog Ser* **92**: 205–219.

Eisen, M.B., P.T. Spellman, P.O. Brown, D. Botstein. (1998) Cluster analysis and display of genome-wide expression patterns. *Proc Natl Acad Sci USA* **95**: 14863-14868.

Fields, M.W., T. Yan, S.K. Rhee, S.L. Carroll, P.M. Jardine, D.B. Watson, C.S. Criddle, J. Zhou. (2005) Impacts on microbial communities and cultivable isolates from groundwater contaminated with high levels of nitric acid-uranium waste. *FEMS Microbiol Ecol* **53**: 417-428.

Gu, B, T.J. Phelps, L. Liang, M.J. Dickey, Y. Roh , B.L. Kinsall, A.V. Palumbo, G.K. Jacobs. **(**1999) Biogeochemical dynamics in zero-valent iron columns: Implications for permeable reactive barriers. *Environ Sci Technol* **33**: 2170-2177.

Gu, B.H. D.B. Watson, L.Y. Wu, D.H. Phillips, D.C. White, J. Zhou. (2002) Microbiological characteristics in a zero-valent iron reactive barrier. *Environ Monit Assess* **77**: 293-309.

He, Z., T.J. Gentry, C.W. Schadt, L. WU, J. Liebich, S.C. Chong, Z. Huang, W. Wu, B. Gu, P. Jardine, C. Criddle, J. Zhou. (2007) Geochip: A comprehensive microarray for investigating biogeochemical, ecological and environmental processes. *ISME J* **1**: 67-77.

Hotelling, H. (1936) Relations between two sets of variates. *Biometrika* **28**: 321-377.

Hua, B., H. Xu, J. Terry, B. Deng. (2006) Kinetics of Uranium(VI) Reduction by hydrogen sulfide in anoxic aqueous systems. *Environ Sci Technol* **40**: 4666-4671.

Leaphart, A.B., C.R. Lovell. (2001) Recovery and analysis of formyltetrahydrofolate synthetase gene sequences from natural populations of acetogenic bacteria. *Appl Environ Microbiol* **67**: 1392-1395.

Lenczewski, M., P.Jardine, L.McKay, A. Layton. (2003) Natural attenuation of trichloroethylene in fractured shale bedrock. *J Contam Hydrol* **64**: 151-168.

Lloyd, J.R., H.F. Nolting, V.A. Sole, K. Bosecker. (1998) Technetium reduction and precipitation by sulfate-reducing bacteria. *Geomicrobiol J* **15**: 45-58.

Lovley, D.R., E.J.P. Phillips. (1992) Reduction of uranium by *Desulfovibrio desulfuricans*. *Appl Environ Microbiol* **58**: 850–56.

Mantel, N. (1967) The detection of disease clustering and a generalized regression approach. *Cancer Res* **27**: 209-220.

McCune, B. and M.J. Mefford. (1999) PC-ORD. Multivariate Analysis of Ecological Data. Version 5.0 MjM Software, Gleneden Beach, Oregon, U.S.A.

Nies, D.H. (2003) Efflux-mediated heavy metal resistance in prokaryotes. *FEMS Microbiol Rev* **27**: 313-339.

Oak Ridge National Laboratory (2008). Integrated Field-scale Subsurface Research Challenge. URL www.esd.ornl.gov/orifrc/

Palumbo, A.V., J.C. Schryver, M.W. Fields, C.E. Bagwell, J.Z. Zhou, T. Yan, X. Liu, C.C. Brandt. (2004) Coupling of functional gene diversity and geochemical data from environmental samples. *Appl Environ Microbiol* **70**: 6525-6534.

Payne, R.B., D.A. Gentry,,B.J. Rapp-Giles, L. Casalot, J.D. Wall. (2002) Uranium reduction by *Desulfovibrio desulfuricans* strain G20 and a cytochrome c3 mutant. *Appl Environ Microbiol* **68**: 3129-3132.

Phillips, D.H., B. Gu, D.B. Watson, Y. Roh, L. Liang, S.Y. Lee. (2000) Performance evaluation of a zerovalent iron reactive barrier: Mineralogical characteristics. *Environ Sci Technol* **34**: 4169-4176.

R Development Core Team. (2008) R: A Language and Environment for Statistical Computing, URL www.R-project.org

Rhee, S. K., X. D. Liu, L. Y. Wu, S. C. Chong, X. F. Wan, and J. Z. Zhou. (2004) Detection of genes involved in biodegradation and biotransformation in microbial communities by using 50-mer oligonucleotide microarrays. *Appl Environ Microbiol* **70:** 4303–4317.

Spain, A.M., A.D. Peacock, J.D. Istok, M.S. Elshahed, F.Z. Najar, B.A. Roe, D.C. White, L.R. Krumholz. (2007) Identification and isolation of a Castellaniella species important during biostimulation of an acidic nitrate- and uranium-contaminated aquifer. *Appl Environ Microbiol* **73**: 4892-904.

ter Braak C.J.F. (1988) CANOCO—an extension of DECORANA to analyze species–environment relationships. *Vegetatio* **75**: 159–160.

Tiquia, S.M., L. Wu, S.C. Chong, S. Passovets, D. Xu, Y. Xu, and J. Zhou. (2004) Evaluation of 50-mer oligonucleotide arrays for detecting microbial populations in environmental samples. *BioTechniques* **36**: 664-675.

Verdnik, D., S. Handran, and S. Pickett. **(**2002) Key considerations for accurate microarray scanning and image analysis, p. 83–98. *In* G. Kamberrova and S. Shah (ed.), DNA array image analysis nuts & bolts. DNA Press, Eagleville, Pa.

Walter, E.G., C.M. Thomas, J.P Ibbotson, D.E. Taylor. (1991) Transcriptional analysis, translational analysis, and sequence of the kilA-tellurite resistance region of plasmid RK2Te^{r}. *J Bacteriol* **173**: 1111-1119.

Wu, L., X. Liu, C.W. Schadt, J. Zhou. (2006) Microarray-based analysis of subnanogram quantities of microbial community DNAs by using whole-community genome amplification. *Appl Envion Microbiol* **72**: 4931-4941.

Yan, T., M.W. Fields, L. Wu, Y. Zu, J.M. Tiedje, J. Zhou. (2003) Molecular diversity and characterization of nitrite reductase gene fragments (*nir*K and *nir*S) from nitrate- and uranium-contaminated groundwater. *Environ Microbiol* **5**: 13-24.

Zhou, J. Z., M. R. Fries, J. C. Cheesanford, and J. M. Tiedje. **(**1995) Phylogenetic analyses of a new group of denitrifiers capable of anaerobic growth on toluene and description of *Azoarcus tolulyticus* sp. nov. *Int J Syst Bacteriol* **45:** 500-506.

Zhou, P., B. Gu. (2005) Extraction of oxidized and reduced forms of uranium from contaminated soils: Effects of carbonate concentration and pH. *Environ Sci Technol* **39:** 4435-4440.

Table 1. Geochemical variables measured from each FRC monitoring well.

	FRC Area Location[a]	pH	Al (mg/l)	Cl (mg/l)	Ni (mg/l)	Nitrate (mg/l)	Sulfate (mg/l)	U (mg/L)	Tc (pCi/l)
FW300	B	6.7	0.2	2.4	0.0	2.6	6.4	0.0	0.0
FW003	2	6.0	0.4	124.7	0.0	1015.0	16.3	0.1	141.0
FW021	1	3.4	398.0	220.2	11.9	8823.0	122.1	12.2	30974.0
FW010	3	3.5	1120.0	686.4	15.7	43019.0	8.3	0.2	7190.0
FW024	3	3.6	527.4	281.4	12.5	8481.0	987.1	44.8	36956.0
TPB16	2	6.3	0.0	78.3	0.0	25.4	116.1	1.2	886.0

[a]B = background

Table 2. Mantel test r-value results for environmental variables and gene diversity detected by GeoChip in FRC groundwater.

Geochemical Variable	P-Value[a]	R-value
pH	0.11111	-0.1538
aluminum	0.74775	-0.0603
Chloride	0.08008	-0.1451
nickel	0.1982	0.113
nitrate	**0.02703**	**-0.2552**
sulfate	0.36937	-0.1028
uranium	**0.04905**	**-0.233**
Tc	0.07908	-0.1731
all geochemical variables	0.07508	-0.1855

[a] Bolded values are significant (p-value<0.05)

Table 3. Summary of CCA Results from CANOCO.

Axes	**1**	**2**
Eigenvalues	0.490	0.148
Species-environment correlations	0.980	0.994
Cumulative percentage variance:		
of species data	47.4	61.6
of species-env relation	64.6	84.0
Sum of all eigenvalues	1.035	
Sum of all canonical eigenvalues	0.759	
Summary of Monte Carlo test		
Test of significance of first canonical axis	0.490	
F-ratio	1.800	
P-value	0.077	
Test of significance of all canonical axes	0.759	
F-ratio	1.833	
P-value	0.041	

Fig. 1. Relative abundance of all functional gene categories detected by the FGA. The total number of genes detected for each well was used to calculate the relative abundance of each category.

Fig. 2. Hierarchical cluster analysis of gene diversity based on hybridization signal intensities. The color red indicates the level of signal intensity; black indicates no hybridization above the background level. (a) Nitrite reductases (*nirK* and *nirS),* (b) Sulfite-reductases (*dsrAB*), (c) Genes involved in metal transport and resistance, (d) Genes involved in carbon fixation, (e) Genes involved in organic contaminant degradation.

Fig. 3. Canonical correspondence analysis (CCA) of FGA hybridization signal intensities and groundwater geochemistry variables; technetium and uranium, sulfate and pH. The percent of the variation explained by each axis is shown, and the relationship is significant (p=0.041). These variables were selected based on automatic forward selection of the variables in CANOCO.

Fig. 4. Partitioning of microbial diversity variance among important geochemical variables, technetium and uranium (p=0.086), pH (p=0.175), sulfate (p=.006) , and their interactions. There was zero variance attributed to the interaction of pH and U and Tc, or to the interaction of all variables.

Fig. 1

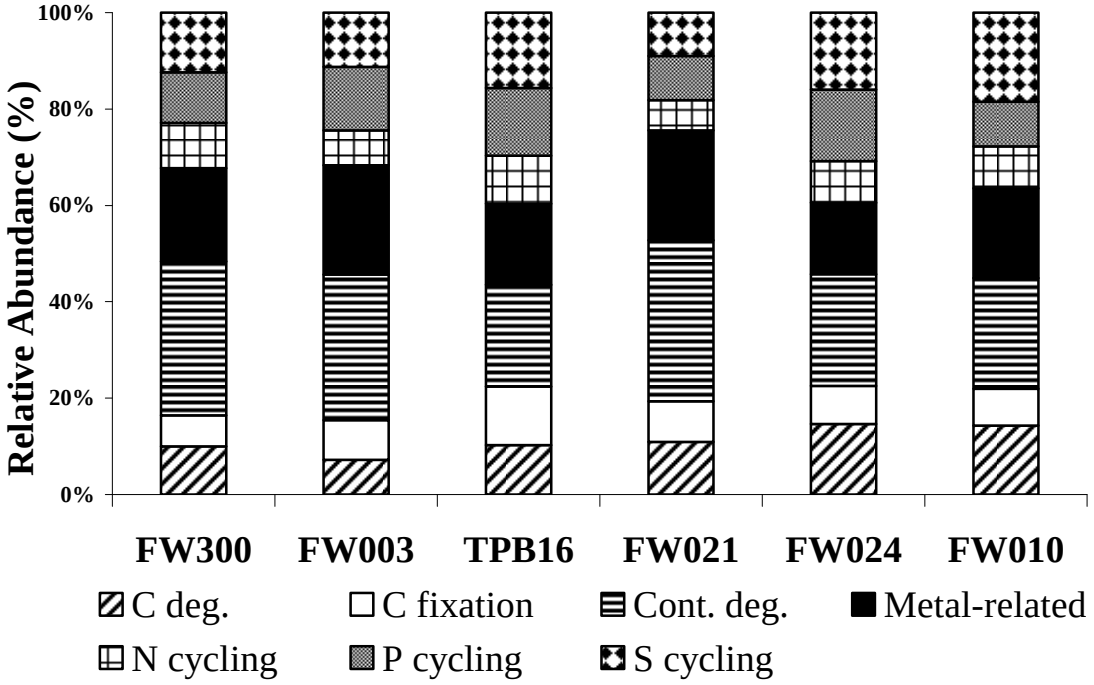
Relative Abundance (%)
100%
80%
60%
40%
20%
0%
FW300
FW003
TPB16
FW021
FW024
FW010
C deg.
C fixation
Cont. deg.
Metal-related
N cycling
P cycling
S cycling

Fig. 2. (a)

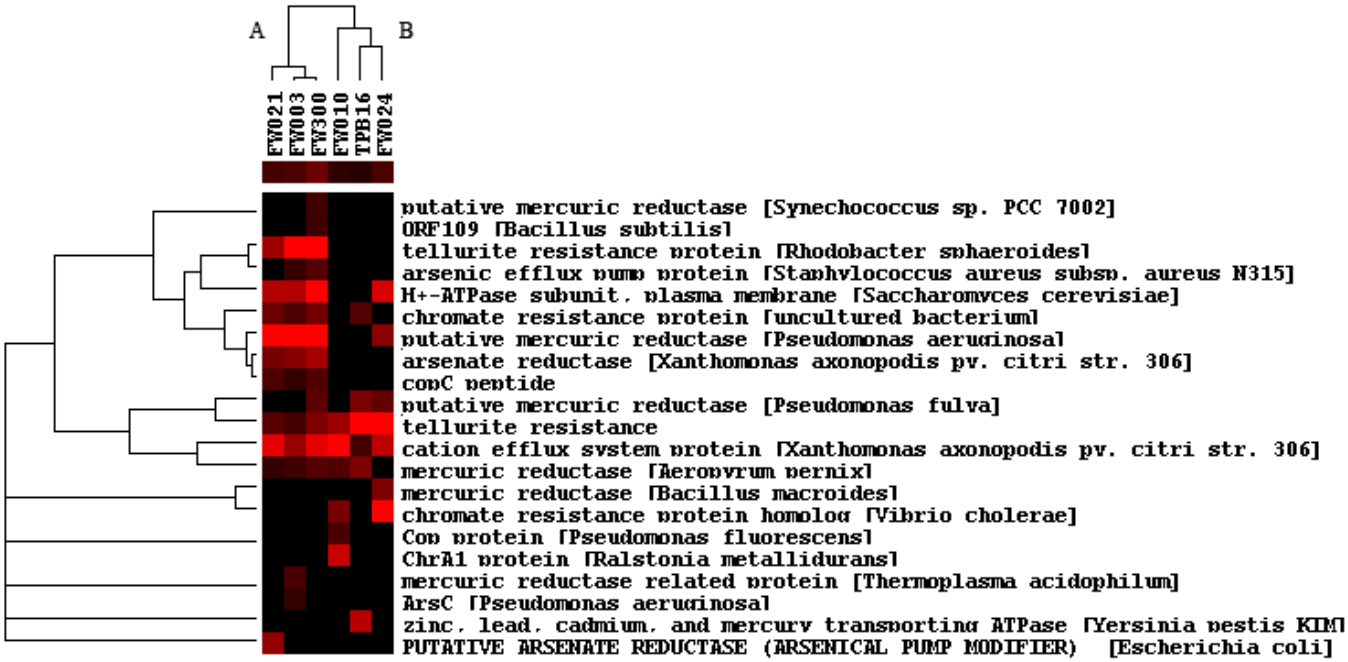
A
B
FW021
FW003
FW300
FW010
TPB16
FW024
putative mercuric reductase [Synechococcus sp. PCC 7002]
ORF109 [Bacillus subtilis]
tellurite resistance protein [Rhodobacter sphaeroides]
arsenic efflux pump protein [Staphylococcus aureus subsp. aureus N315]
H+-ATPase subunit, plasma membrane [Saccharomyces cerevisiae]
chromate resistance protein [uncultured bacterium]
putative mercuric reductase [Pseudomonas aeruginosa]
arsenate reductase [Xanthomonas axonopodis pv. citri str. 306]
copC peptide
putative mercuric reductase [Pseudomonas fulva]
tellurite resistance
cation efflux system protein [Xanthomonas axonopodis pv. citri str. 306]
mercuric reductase [Aeropyrum pernix]
mercuric reductase [Bacillus macroides]
chromate resistance protein homolog [Vibrio cholerae]
Cop protein [Pseudomonas fluorescens]
ChrA1 protein [Ralstonia metallidurans]
mercuric reductase related protein [Thermoplasma acidophilum]
ArsC [Pseudomonas aeruginosa]
zinc, lead, cadmium, and mercury transporting ATPase [Yersinia pestis KIM]
PUTATIVE ARSENATE REDUCTASE (ARSENICAL PUMP MODIFIER) [Escherichia coli]

Fig. 2. (b)

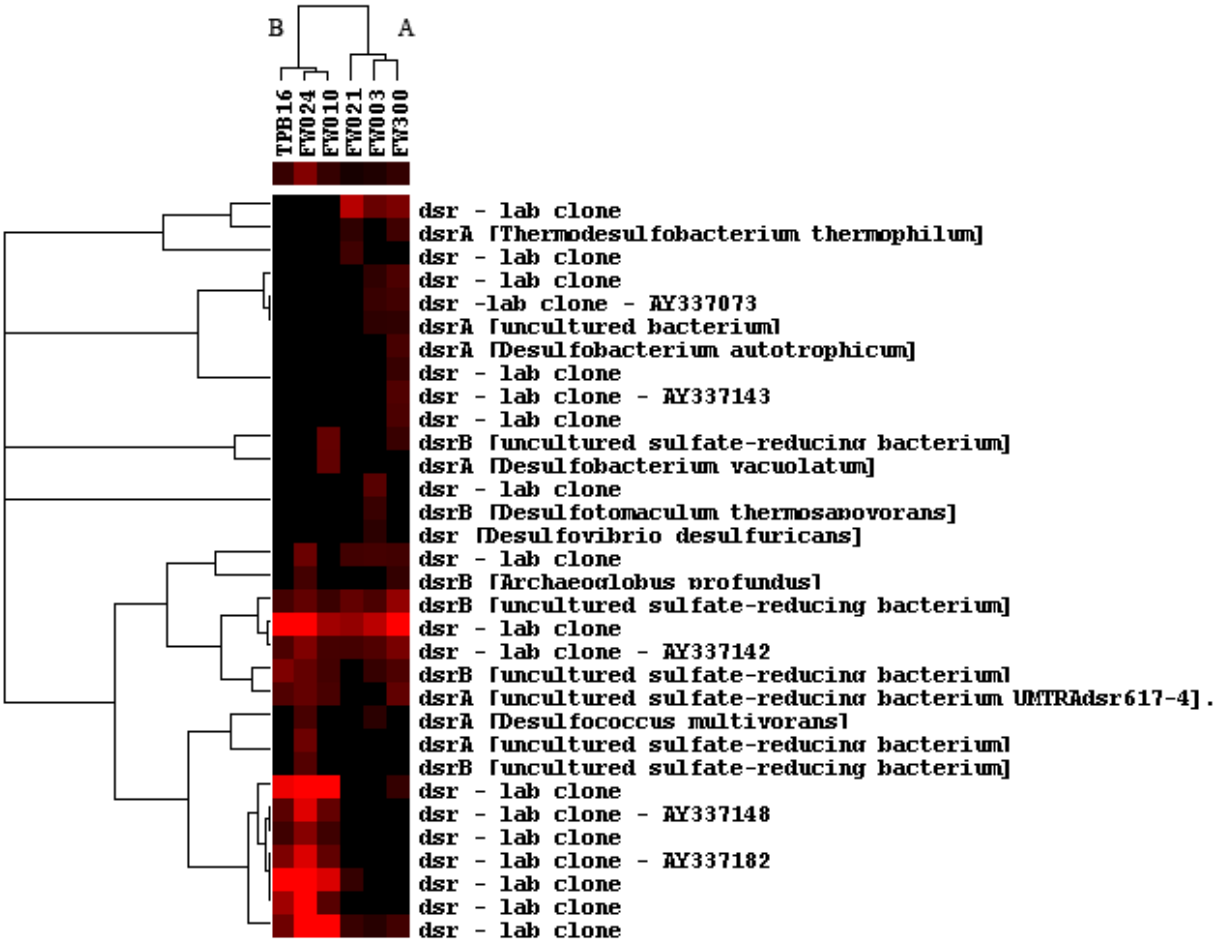
B
A
TPB16
FW024
FW010
FW021
FW003
FW300
dsr - lab clone
dsrA [Thermodesulfobacterium thermophilum]
dsr - lab clone
dsr - lab clone
dsr -lab clone - AY337073
dsrA [uncultured bacterium]
dsrA [Desulfobacterium autotrophicum]
dsr - lab clone
dsr - lab clone - AY337143
dsr - lab clone
dsrB [uncultured sulfate-reducing bacterium]
dsrA [Desulfobacterium vacuolatum]
dsr - lab clone
dsrB [Desulfotomaculum thermosapovorans]
dsr [Desulfovibrio desulfuricans]
dsr - lab clone
dsrB [Archaeoglobus profundus]
dsrB [uncultured sulfate-reducing bacterium]
dsr - lab clone
dsr - lab clone - AY337142
dsrB [uncultured sulfate-reducing bacterium]
dsrA [uncultured sulfate-reducing bacterium UMTRAdsr617-4].
dsrA [Desulfococcus multivorans]
dsrA [uncultured sulfate-reducing bacterium]
dsrB [uncultured sulfate-reducing bacterium]
dsr - lab clone
dsr - lab clone - AY337148
dsr - lab clone
dsr - lab clone - AY337182
dsr - lab clone
dsr - lab clone
dsr - lab clone

Fig. 2. (c)

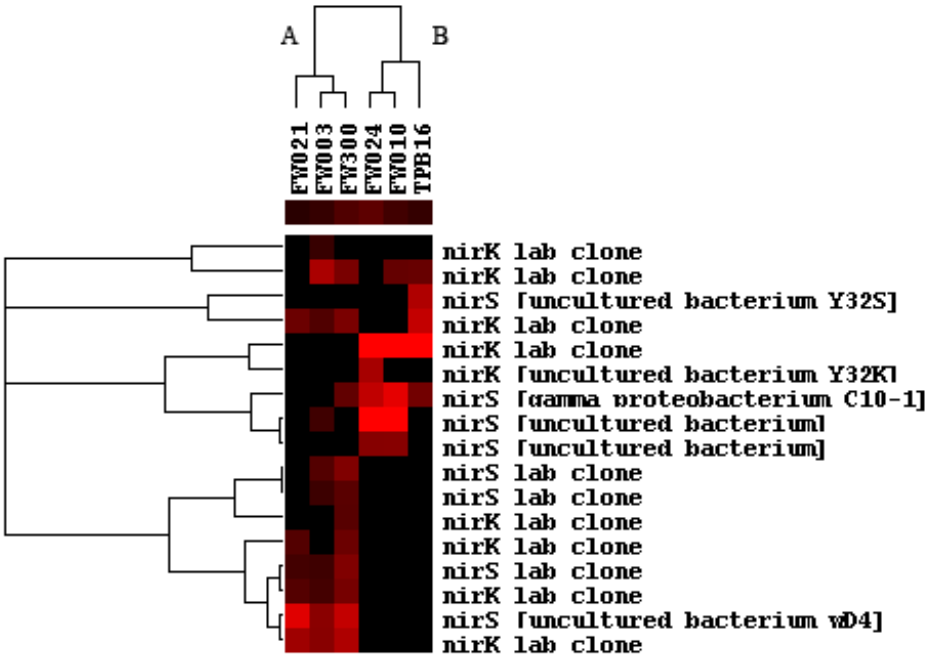
A
B
FW021
FW003
FW300
FW024
FW010
TPB16
nirK lab clone
nirK lab clone
nirS [uncultured bacterium Y32S]
nirK lab clone
nirK lab clone
nirK [uncultured bacterium Y32K]
nirS [gamma proteobacterium C10-1]
nirS [uncultured bacterium]
nirS [uncultured bacterium]
nirS lab clone
nirS lab clone
nirK lab clone
nirK lab clone
nirS lab clone
nirK lab clone
nirS [uncultured bacterium wD4]
nirK lab clone

Fig. 2. (d)

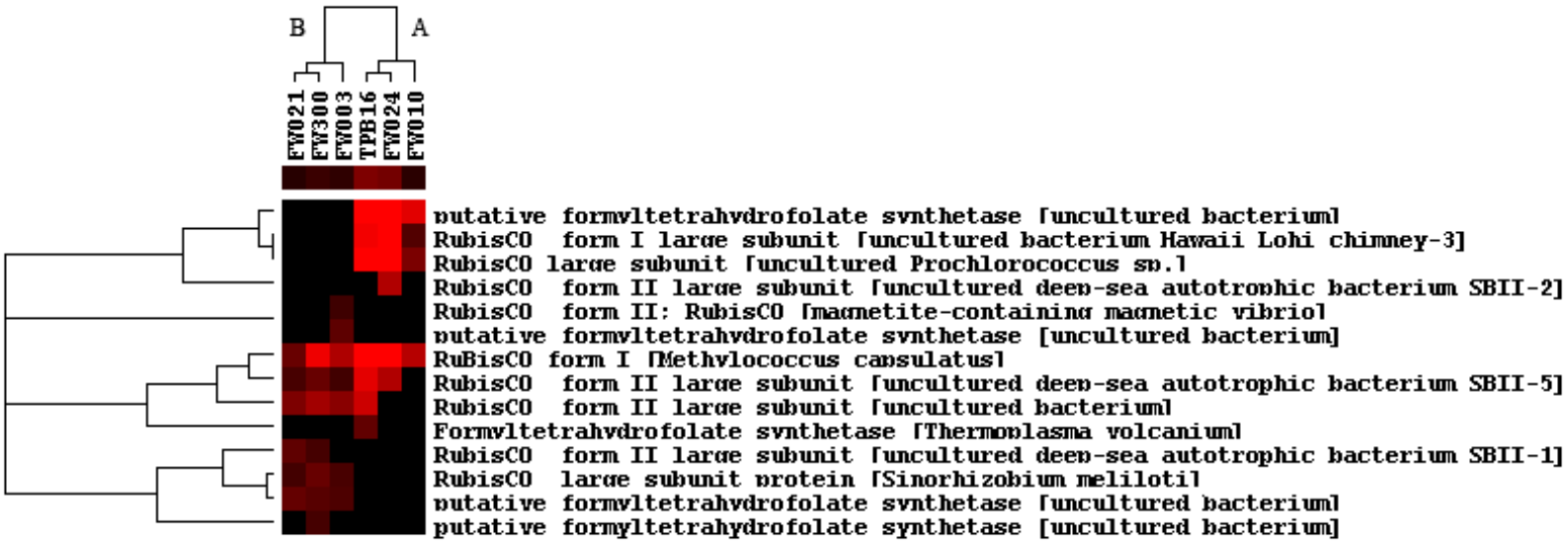
B
A
FW021
FW300
FW003
TPB16
FW024
FW010
putative formyltetrahydrofolate synthetase [uncultured bacterium]
RubisCO form I large subunit [uncultured bacterium Hawaii Lohi chimney-3]
RubisCO large subunit [uncultured Prochlorococcus sp.]
RubisCO form II large subunit [uncultured deep-sea autotrophic bacterium SBII-2]
RubisCO form II: RubisCO [magnetite-containing magnetic vibrio]
putative formyltetrahydrofolate synthetase [uncultured bacterium]
RuBisCO form I [Methylococcus capsulatus]
RubisCO form II large subunit [uncultured deep-sea autotrophic bacterium SBII-5]
RubisCO form II large subunit [uncultured bacterium]
Formyltetrahydrofolate synthetase [Thermoplasma volcanium]
RubisCO form II large subunit [uncultured deep-sea autotrophic bacterium SBII-1]
RubisCO large subunit protein [Sinorhizobium meliloti]
putative formyltetrahydrofolate synthetase [uncultured bacterium]
putative formyltetrahydrofolate synthetase [uncultured bacterium]

Fig. 2.(e)

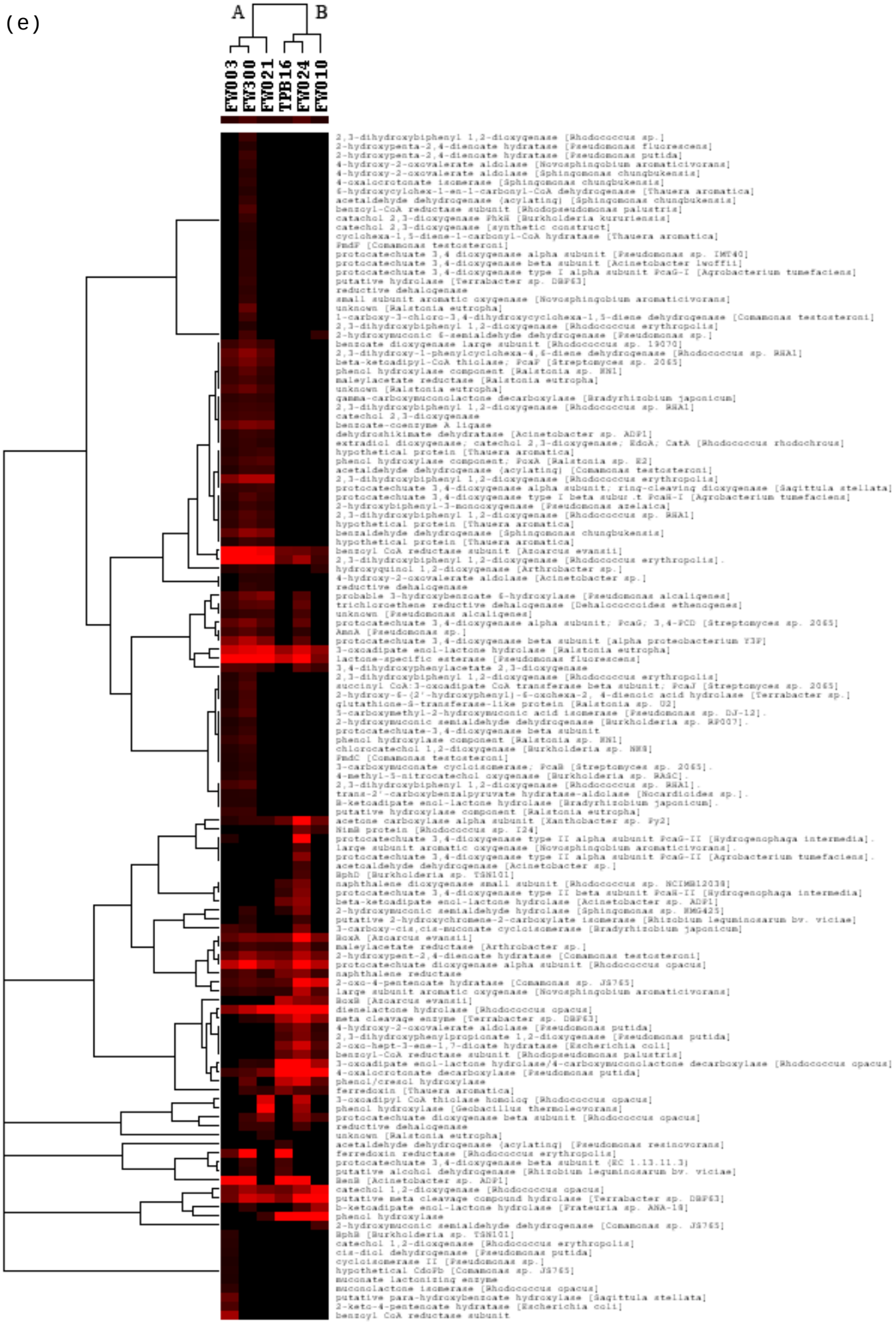
A
B
FW003
FW300
FW021
TPB16
FW024
FW010
2,3-dihydroxybiphenyl 1,2-dioxygenase [Rhodococcus sp.]
2-hydroxypenta-2,4-dienoate hydratase [Pseudomonas fluorescens]
2-hydroxypenta-2,4-dienoate hydratase [Pseudomonas putida]
4-hydroxy-2-oxovalerate aldolase [Novosphingobium aromaticivorans]
4-hydroxy-2-oxovalerate aldolase [Sphingomonas chunqbukensis]
4-oxalocrotonate isomerase [Sphingomonas chunqbukensis]
6-hydroxycyclohex-1-en-1-carbonyl-CoA dehydrogenase [Thauera aromatica]
acetaldehyde dehydrogenase (acylating) [Sphingomonas chunqbukensis]
benzoyl-CoA reductase subunit [Rhodopseudomonas palustris]
catechol 2,3-dioxygenase PhxB [Burkholderia kururiensis]
catechol 2,3-dioxygenase [synthetic construct]
cyclohexa-1,5-diene-1-carbonyl-CoA hydratase [Thauera aromatica]
PmdF [Comamonas testosteroni]
protocatechuate 3,4 dioxygenase alpha subunit [Pseudomonas sp. IMT40]
protocatechuate 3,4-dioxygenase beta subunit [Acinetobacter lwoffii]
protocatechuate 3,4-dioxygenase type I alpha subunit PcaG-I [Agrobacterium tumefaciens]
putative hydrolase [Terrabacter sp. DBF63]
reductive dehalogenase
small subunit aromatic oxygenase [Novosphingobium aromaticivorans]
unknown [Ralstonia eutropha]
1-carboxy-3-chloro-3,4-dihydroxycyclohexa-1,5-diene dehydrogenase [Comamonas testosteroni]
2,3-dihydroxybiphenyl 1,2-dioxygenase [Rhodococcus erythropolis]
2-hydroxymuconic 6-semialdehyde dehydrogenase [Pseudomonas sp.]
benzoate dioxygenase large subunit [Rhodococcus sp. 19070]
2,3-dihydroxy-1-phenylcyclohexa-4,6-diene dehydrogenase [Rhodococcus sp. RHA1]
beta-ketoadipyl-CoA thiolase; PcaF [Streptomyces sp. 2065]
phenol hydroxylase component [Ralstonia sp. HN1]
maleylacetate reductase [Ralstonia eutropha]
unknown [Ralstonia eutropha]
gamma-carboxymuconolactone decarboxylase [Bradyrhizobium japonicum]
2,3-dihydroxybiphenyl 1,2-dioxygenase [Rhodococcus sp. RHA1]
catechol 2,3-dioxygenase
benzoate-coenzyme A ligase
dehydroshikimate dehydratase [Acinetobacter sp. ADP1]
extradiol dioxygenase; catechol 2,3-dioxygenase; EdoA; CatA [Rhodococcus rhodochrous]
hypothetical protein [Thauera aromatica]
phenol hydroxylase component; PoxA [Ralstonia sp. E2]
acetaldehyde dehydrogenase (acylating) [Comamonas testosteroni]
2,3-dihydroxybiphenyl 1,2-dioxygenase [Rhodococcus erythropolis]
protocatechuate 3,4-dioxygenase alpha subunit; ring-cleaving dioxygenase [Saqittula stellata]
protocatechuate 3,4-dioxygenase type I beta subunit PcaH-I [Agrobacterium tumefaciens]
2-hydroxybiphenyl-3-monooxygenase [Pseudomonas azelaica]
2,3-dihydroxybiphenyl 1,2-dioxygenase [Rhodococcus sp. RHA1]
hypothetical protein [Thauera aromatica]
benzaldehyde dehydrogenase [Sphingomonas chunqbukensis]
hypothetical protein [Thauera aromatica]
benzoyl CoA reductase subunit [Azoarcus evansii]
2,3-dihydroxybiphenyl 1,2-dioxygenase [Rhodococcus erythropolis].
hydroxyquinol 1,2-dioxygenase [Arthrobacter sp.]
4-hydroxy-2-oxovalerate aldolase [Acinetobacter sp.]
reductive dehalogenase
probable 3-hydroxybenzoate 6-hydroxylase [Pseudomonas alcaligenes]
trichloroethene reductive dehalogenase [Dehalococcoides ethenogenes]
unknown [Pseudomonas alcaligenes]
protocatechuate 3,4-dioxygenase alpha subunit; PcaG; 3,4-PCD [Streptomyces sp. 2065]
AmnA [Pseudomonas sp.]
protocatechuate 3,4-dioxygenase beta subunit [alpha proteobacterium Y3P]
3-oxoadipate enol-lactone hydrolase [Ralstonia eutropha]
lactone-specific esterase [Pseudomonas fluorescens]
3,4-dihydroxyphenylacetate 2,3-dioxygenase
2,3-dihydroxybiphenyl 1,2-dioxygenase [Rhodococcus erythropolis]
succinyl CoA:3-oxoadipate CoA transferase beta subunit; PcaJ [Streptomyces sp. 2065]
2-hydroxy-6-(2'-hydroxyphenyl)-6-oxohexa-2, 4-dienoic acid hydrolase [Terrabacter sp.]
glutathione-S-transferase-like protein [Ralstonia sp. U2]
5-carboxymethyl-2-hydroxymuconic acid isomerase [Pseudomonas sp. DJ-12].
2-hydroxymuconic semialdehyde dehydrogenase [Burkholderia sp. RP007].
protocatechuate-3,4-dioxygenase beta subunit
phenol hydroxylase component [Ralstonia sp. HN1]
chlorocatechol 1,2-dioxygenase [Burkholderia sp. NH8]
PmdC [Comamonas testosteroni]
3-carboxymuconate cycloisomerase; PcaB [Streptomyces sp. 2065].
4-methyl-5-nitrocatechol oxygenase [Burkholderia sp. RASC].
2,3-dihydroxybiphenyl 1,2-dioxygenase [Rhodococcus sp. RHA1].
trans-2'-carboxybenzalpyruvate hydratase-aldolase [Nocardioides sp.].
B-ketoadipate enol-lactone hydrolase [Bradyrhizobium japonicum].
putative hydroxylase component [Ralstonia eutropha]
acetone carboxylase alpha subunit [Xanthobacter sp. Py2]
NimB protein [Rhodococcus sp. I24]
protocatechuate 3,4-dioxygenase type II alpha subunit PcaG-II [Hydrogenophaga intermedia].
large subunit aromatic oxygenase [Novosphingobium aromaticivorans].
protocatechuate 3,4-dioxygenase type II alpha subunit PcaG-II [Agrobacterium tumefaciens].
acetoaldehyde dehydrogenase [Acinetobacter sp.]
BphD [Burkholderia sp. TSN101]
naphthalene dioxygenase small subunit [Rhodococcus sp. NCIMB12038]
protocatechuate 3,4-dioxygenase type II beta subunit PcaH-II [Hydrogenophaga intermedia]
beta-ketoadipate enol-lactone hydrolase [Acinetobacter sp. ADP1]
2-hydroxymuconic semialdehyde hydrolase [Sphingomonas sp. HMG425]
putative 2-hydroxychromene-2-carboxylate isomerase [Rhizobium leguminosarum bv. viciae]
3-carboxy-cis,cis-muconate cycloisomerase [Bradyrhizobium japonicum]
BoxA [Azoarcus evansii]
maleylacetate reductase [Arthrobacter sp.]
2-hydroxypent-2,4-dienoate hydratase [Comamonas testosteroni]
protocatechuate dioxygenase alpha subunit [Rhodococcus opacus]
naphthalene reductase
2-oxo-4-pentenoate hydratase [Comamonas sp. JS765]
large subunit aromatic oxygenase [Novosphingobium aromaticivorans]
BoxB [Azoarcus evansii]
dienelactone hydrolase [Rhodococcus opacus]
meta cleavage enzyme [Terrabacter sp. DBF63]
4-hydroxy-2-oxovalerate aldolase [Pseudomonas putida]
2,3-dihydroxyphenylpropionate 1,2-dioxygenase [Pseudomonas putida]
2-oxo-hept-3-ene-1,7-dioate hydratase [Escherichia coli]
benzoyl-CoA reductase subunit [Rhodopseudomonas palustris]
3-oxoadipate enol-lactone hydrolase/4-carboxymuconolactone decarboxylase [Rhodococcus opacus]
4-oxalocrotonate decarboxylase [Pseudomonas putida]
phenol/cresol hydroxylase
ferredoxin [Thauera aromatica]
3-oxoadipyl CoA thiolase homolog [Rhodococcus opacus]
phenol hydroxylase [Geobacillus thermoleovorans]
protocatechuate dioxygenase beta subunit [Rhodococcus opacus]
reductive dehalogenase
unknown [Ralstonia eutropha]
acetaldehyde dehydrogenase (acylating) [Pseudomonas resinovorans]
ferredoxin reductase [Rhodococcus erythropolis]
protocatechuate 3,4-dioxygenase beta subunit (EC 1.13.11.3)
putative alcohol dehydrogenase [Rhizobium leguminosarum bv. viciae]
BenB [Acinetobacter sp. ADP1]
catechol 1,2-dioxygenase [Rhodococcus opacus]
putative meta cleavage compound hydrolase [Terrabacter sp. DBF63]
b-ketoadipate enol-lactone hydrolase [Frateuria sp. ANA-18]
phenol hydroxylase
2-hydroxymuconic semialdehyde dehydrogenase [Comamonas sp. JS765]
BphB [Burkholderia sp. TSN101]
catechol 1,2-dioxygenase [Rhodococcus erythropolis]
cis-diol dehydrogenase [Pseudomonas putida]
cycloisomerase II [Pseudomonas sp.]
hypothetical CdcFb [Comamonas sp. JS765]
muconate lactonizing enzyme
muconolactone isomerase [Rhodococcus opacus]
putative para-hydroxybenzoate hydroxylase [Saqittula stellata]
2-keto-4-pentenoate hydratase [Escherichia coli]
benzoyl CoA reductase subunit

Fig. 3.

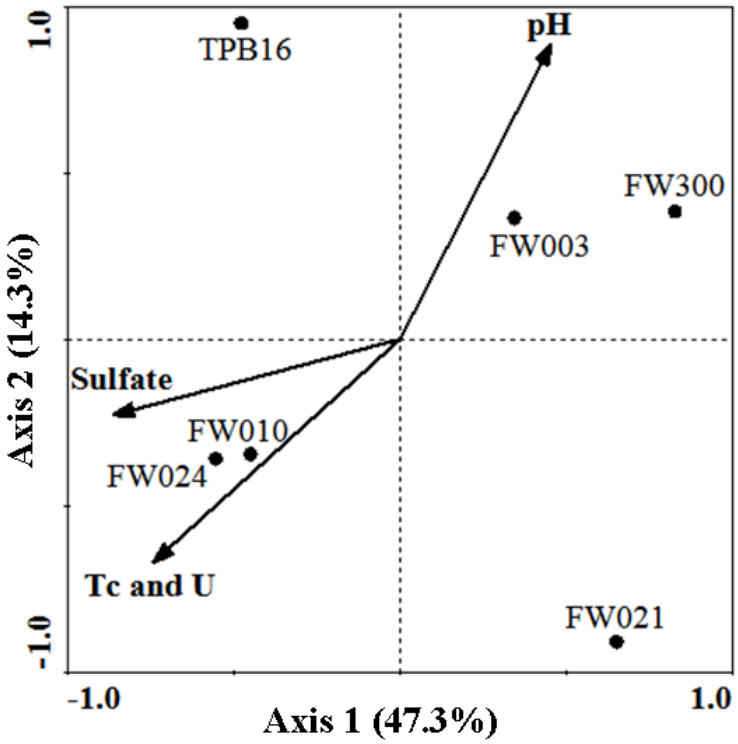
1.0
TPB16
pH
FW300
FW003
Axis 2 (14.3%)
Sulfate
FW010
FW024
Tc and U
FW021
-1.0
-1.0
1.0
Axis 1 (47.3%)

Fig. 4.